# Electronic Supplementary Information

## Flexible and Fragmentable Tandem Photosensitive Nanocrystal Skins

S. Akhavan,[a] C. Uran,[a] B. Bozok,[a] K. Gungor,[a] Y. Kelestemur,[a] V. Lesnyak,[b,c] N. Gaponik,[b] A. Eychmüller[b] and H. V. Demir[a,d]

[a]*UNAM–Institute of Materials Science and Nanotechnology, Department of Electrical and Electronics Engineering and Department of Physics, Bilkent University, Ankara, 06800, Turkey*

[b]*Physical Chemistry, Technische Universität Dresden, Dresden, 01062, Germany*

[c]*Department of Nanochemistry, Istituto Italiano di Tecnologia, Genova, 16163, Italy*

[d]*School of Electrical and Electronic Engineering and School of Physical and Mathematical Sciences, Nanyang Technological University, Singapore, 639798, Singapore*

**Corresponding Author**

E-mail: volkan@stanfordalumni.org

**S1. Absorption and photoluminescence spectra of CdTe and CdHgTe NCs**

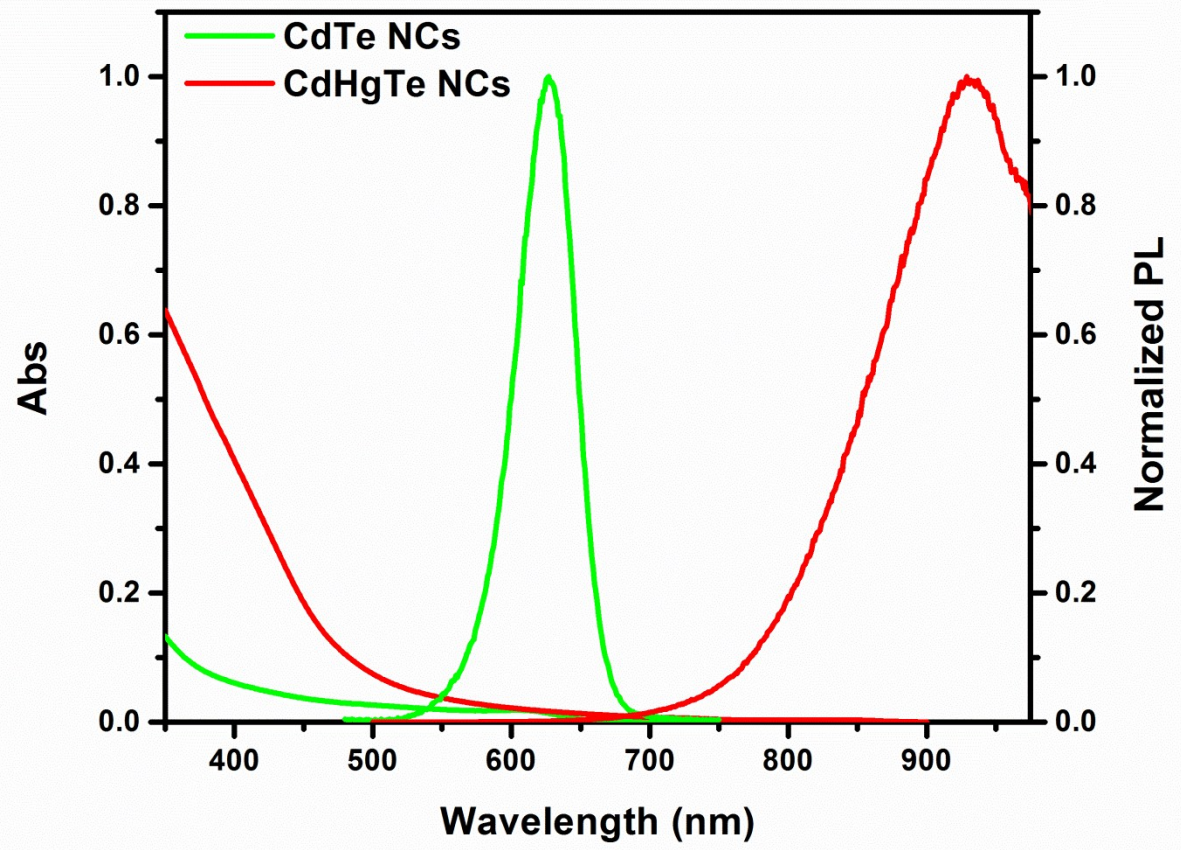


**Figure S1.** Absorption and photoluminescence spectra of the as-synthesized aqueous CdTe and CdHgTe NC solutions.

## S2. XPS spectra of CdTe NCs, CdHgTe NCs and TEM image of CdHgTe NCs.

**(a)**

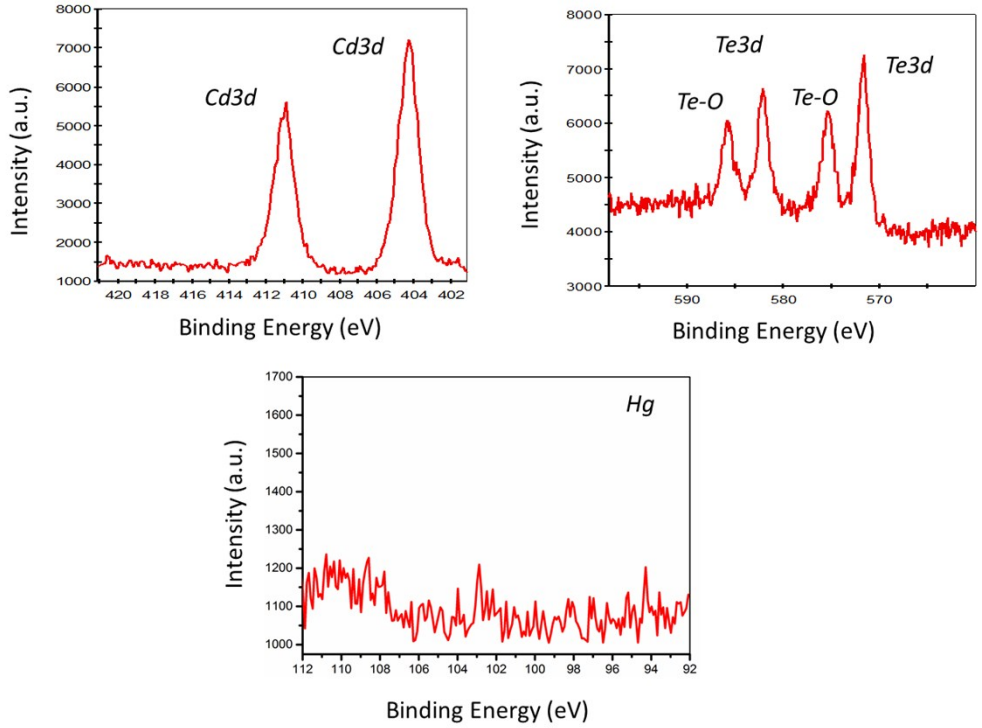


**(b)**

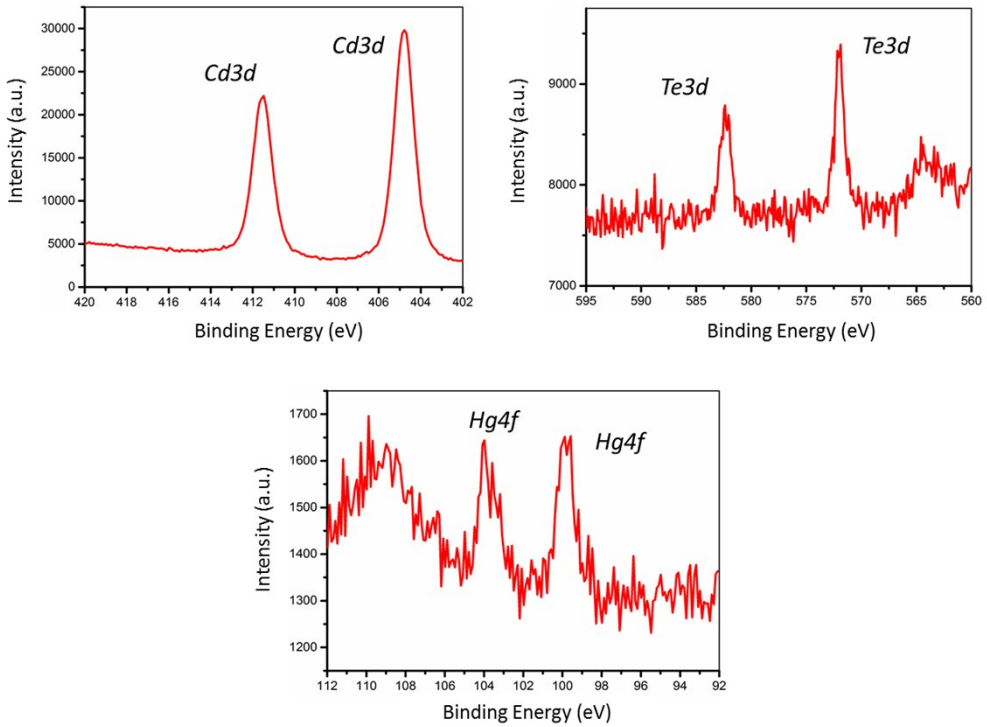

**(c)**

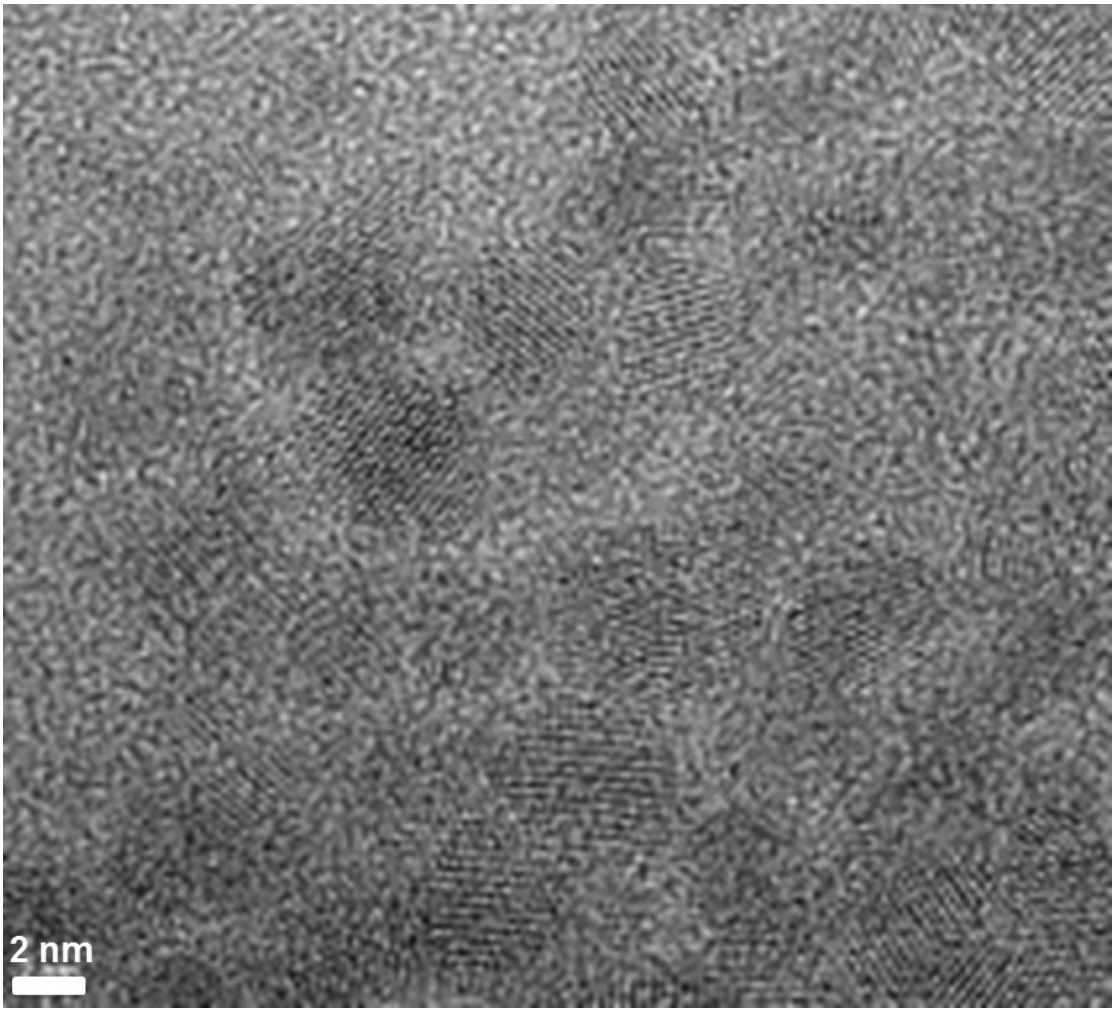


Figure S2. XPS spectra of (a) CdTe NCs, (b) CdHgTe NCs and (c) TEM image of CdHgTe NCs.

**S3. Photosensitive nanocrystal skins fabrication**

ITO coated Kapton substrate was chosen as the bottom electrode. A 300 nm thick ITO film was deposited on Kapton by means of radio frequency (RF)-sputtering. Afterward, it was annealed by a rapid thermal treatment in vacuum at 200 ˚C for 20 min in order to decrease the sheet resistivity of ITO. Then the substrate was exposed to oxygen plasma to create additional hydroxyl groups necessary for the atomic layer deposition (ALD) of the high dielectric constant $HfO_2$ layer.[1] The great challenge in fabricating the tandem PNS is to deposit a thin enough dielectric spacer layer on top of the large-area ITO in order to block charges migrating from the NCs to ITO. Thus, we deposited 50 nm $HfO_2$ via ALD at 200 ˚C. ALD preferentially coats hydrophilic surfaces owing to the usage of pulses of water, which improves the quality of the self-assembled film.[2] Moreover, the encapsulation with $HfO_2$ averts cracking of the plastic substrate in the further fabrication steps. Following that, oppositely charged PDDA and PSS bilayers were coated via a fully computerized dip-coater system. Then, the sample was dipped into the dispersion of the CdHgTe NCs. The coated substrate was subsequently washed with Milli-Q water to remove unbound NCs.[3,4] Finally, immediately after coating the NC monolayer film, the Al contact (8 nm) was deposited via thermal evaporation. The second constituent junction was fabricated similarly on top of the first one but at a different operating temperature of the ALD. Here, we deposited 50 nm $HfO_2$ at low temperatures of 80 ˚C to prevent any damage to the NCs.

**S4. Absorption spectra of NC s in film**

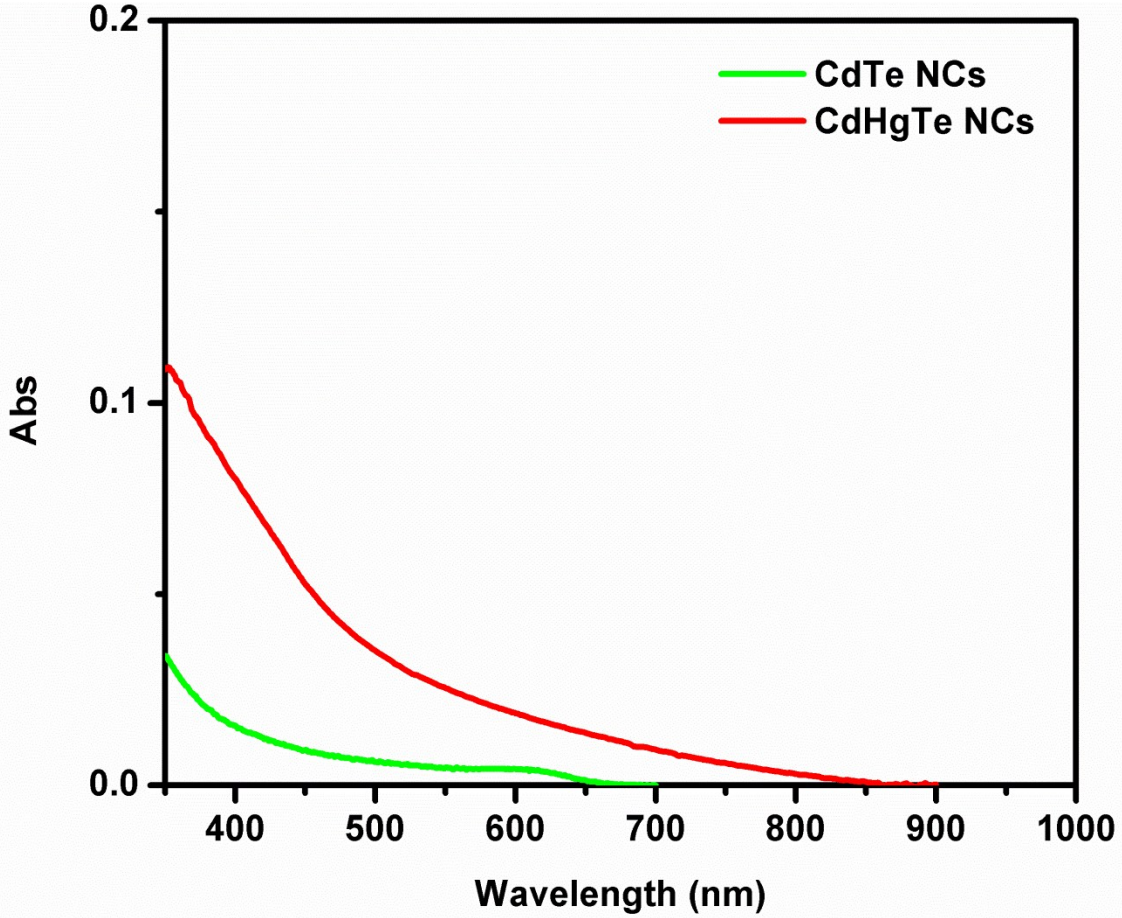


**Figure S4.** Absorption spectra of the CdTe (green) and CdHgTe (red) NC monolayers on glass.

**S5. Transmission spectra of 8 nm aluminum and 35 μm thick polyimide (Kapton)**

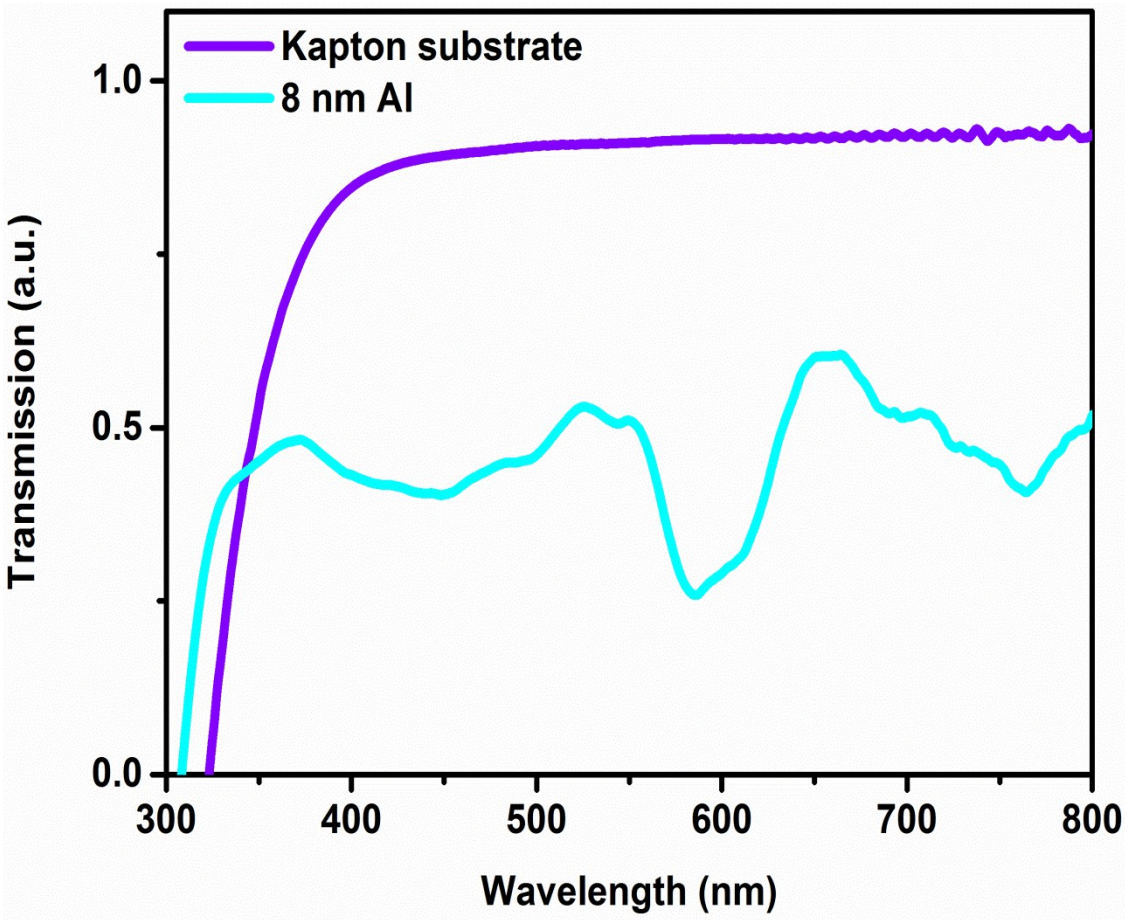


**Figure S5.** Transmission spectra of 8 nm aluminum and 35 μm thick polyimide (Kapton) substrate.

**S6. Investigation of the order of CdgHgTe and CdTe NCs in tandem PNS given the direction of incident light**

To understand the sensitivity improvement mechanism on the optimum device configuration, a model structure is represented. Shown in the Figure S6, $\Phi_A$, $\Phi_B$ and $\Phi_C$ represent the fraction of incident photons absorbed by the active layer A, the active layer B and the layers between these two active layers, respectively.

Total fraction of photons absorbed by the device $\Phi_{device}$ becomes:

$$\Phi_{device} = \Phi_A + (1 - \Phi_A)\Phi_C + (1 - \Phi_A + \Phi_A\Phi_C - \Phi_C)\Phi_B \quad \text{(S1)}$$

Rearranging the terms gives:

$$\Phi_{device} = \Phi_A + \Phi_B + \Phi_C - \Phi_A\Phi_B - \Phi_A\Phi_C - \Phi_B\Phi_C + \Phi_A\Phi_B\Phi_C \quad \text{(S2)}$$

It is seen that changing the order of the layers do not change the device absorption since absorption coefficients of the layers can be interchanged without making any difference in the overall device absorption. However, the overall device sensitivity, $S_{device}$, depends on the absorption coefficients and sensitivity of the layers ($S_A$ and $S_B$ for the sensitivity of active layers A and B, respectively). By neglecting the absorption of the layers between the active layers ($\Phi_C \to 0$), device sensitivity becomes:

$$S_{device} = S_A\Phi_A + S_B(1 - \Phi_A)\Phi_B \quad \text{(S3)}$$

Rearranging the terms we arrive at,

$$S_{device} = S_A\Phi_A + S_B\Phi_B - S_B\Phi_A\Phi_B \quad \text{(S4)}$$

As it can be seen from the given relation (S4), $S_{device}$ is reduced by the sensitivity of the second layer. Subsequently, layers with lower sensitivity should be placed at the bottom junction.

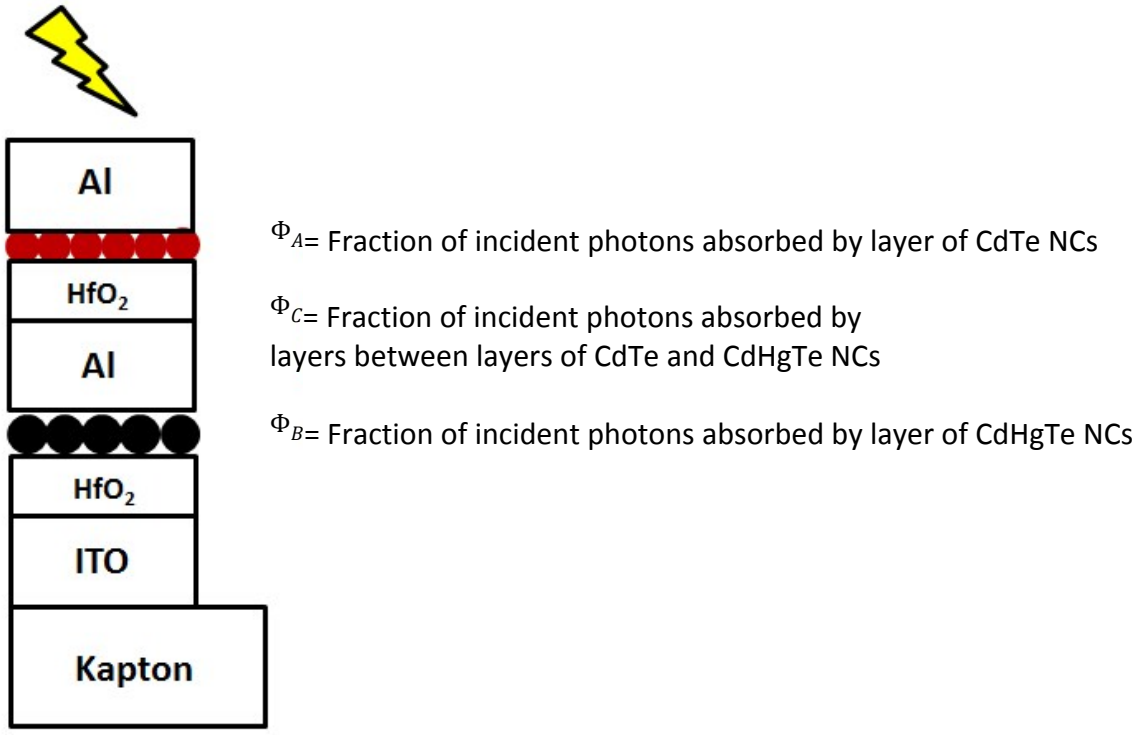


**Figure S6.** Tandem PNS schematics and the direction of incident light.

## S7. Ligand removal

As-synthesized NCs are capped with ligands to impart them with colloidal stability. However, these ligands are insulating and prevent charge transport through the NCs in the solid state at the same time. We have already shown that NCs partially exempted from ligands can be assembled to form a homogeneous, crack-free, randomly close-packed NC thin-film.[5] Partial removal of MPA- and TGA-ligands from CdTe and CdHgTe NCs was monitored through fourier transform infrared (FTIR) spectroscopy. The FTIR study showed no appreciable vibration of the carbon-sulphur (C-S) bond, indicating partial removal of ligands by isopropanol treatment.

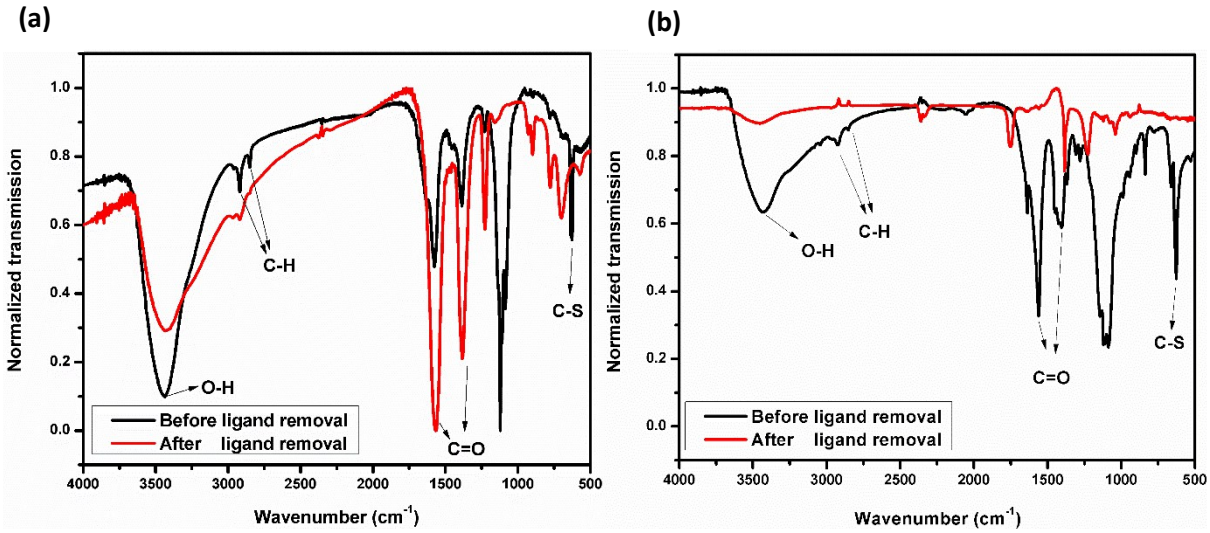


**Figure S7**. Normalized FTIR spectra of (a) CdTe NCs and (b) CdHgTe NCs before and after ligand desorption.

**S8. Reflection, transmission and absorption spectra of photosensitive nanocrystal skins**

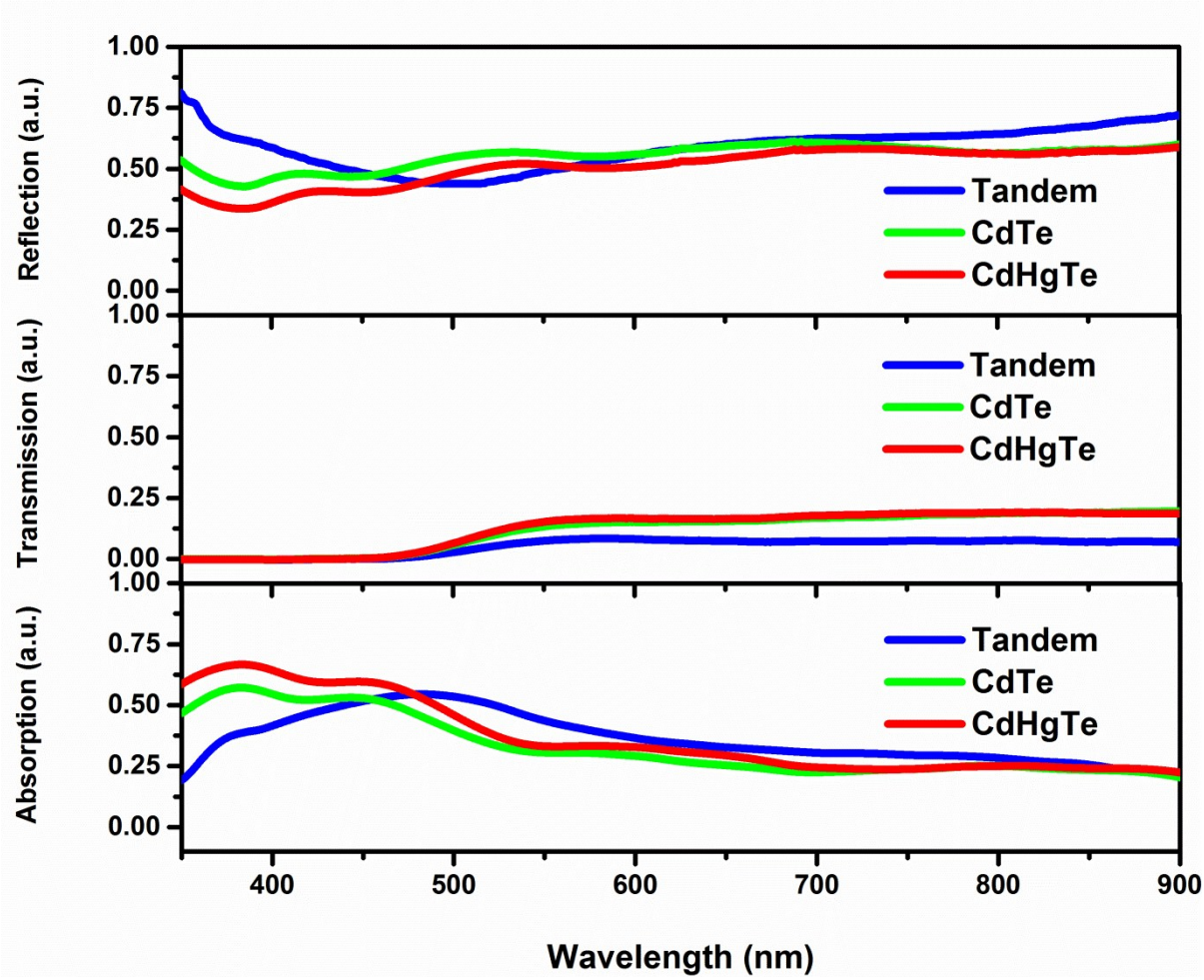


**Figure S8.** Reflection, transmission and absorption spectra of CdTe NC-based PNS, CdHgTe NC-based PNS, and tandem CdTe-CdHgTe NC-based PNS atop 35 μm thick polyimide (Kapton) tape.

**S9. Energy dispersive X-ray (EDX) analysis of single NC layers underneath the electrode on TEM sample**

The cross-sectional images of fabricated tandem PNS are obtained using FEI Tecnai G2 F30 transmission electron microscope (TEM). TEM sample is prepared using FEI Nova 600i Nanolab focused ion beam milling from a completely fabricated device on Kapton film. To prevent milling of the TEM sample during the deposition of the protective platinum layer using ion beam, a thin layer of platinum was deposited using electron beam prior to ion beam platinum deposition.

To demonstrate the presence of single NC layers underneath the electrode, energy dispersive X-ray (EDX) analyses were performed on TEM sample. EDX analyses were carried out in STEM mode using a rectangular window of about 50 nm × 15 nm for the bottom junction (see Fig. S9 a,b). Furthermore, STEM EDX mapping were performed and (c) Al (electrode), (d) CdHgTe NCs layer, (e) $HfO_2$ (dielectric layer), and (f) combination of all materials could be seen. To further characterize the device, (g) high resolution TEM image was taken to demonstrate the interface between the monolayer of NCs and Al contact.

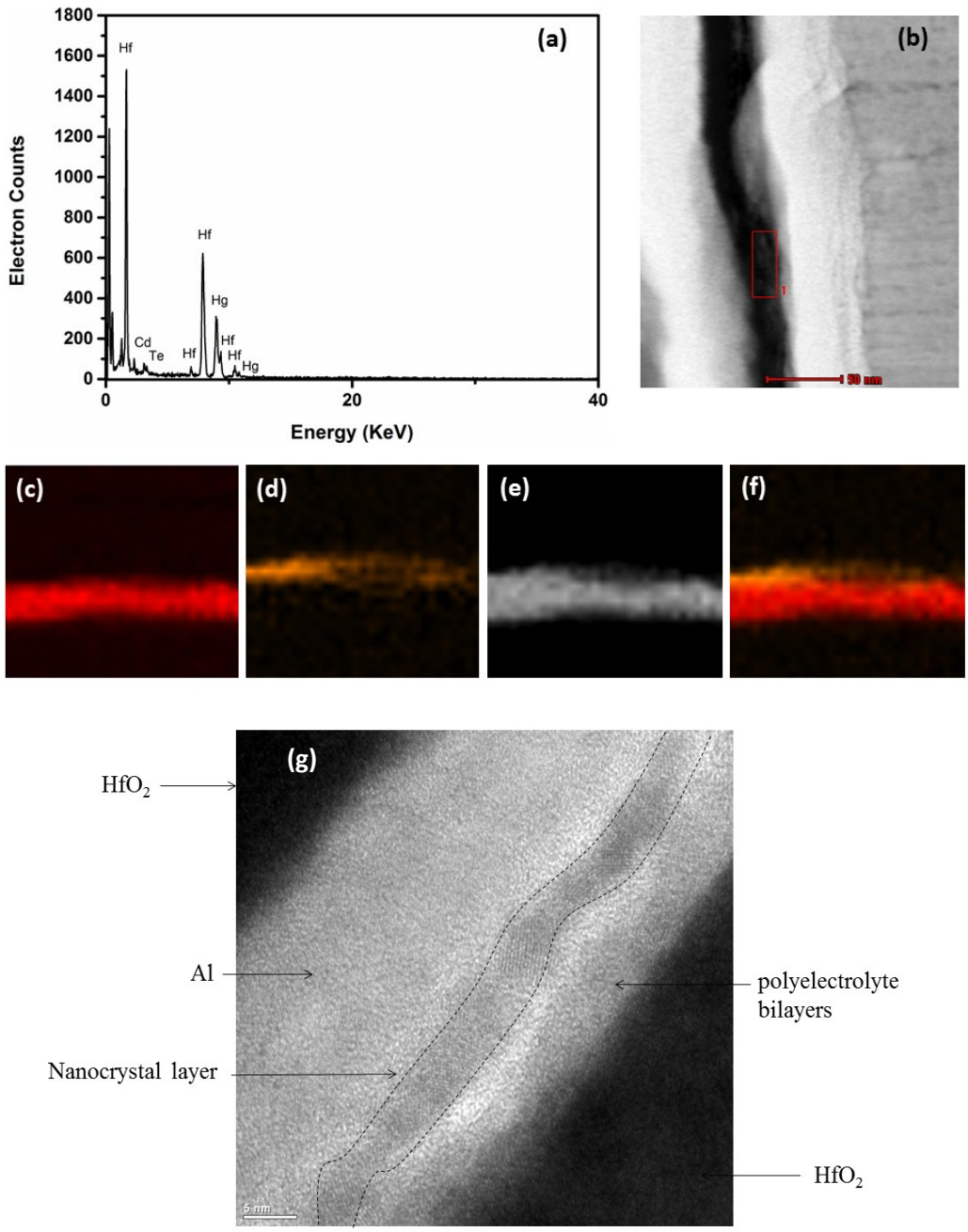


**Figure S9.** (a) EDX spectrum and (b) TEM image of the chosen rectangular window. STEM EDX mapping shows the presence of nanocrystal layer as it can be seen through (c) Al (electrode), (d) CdHgTe NCs layer, (e) $HfO_2$ (dielectric layer), and (f) combination of all materials. (g) High resolution TEM image shows the monolayer of NCs placed underneath the Al electrode and on top of the $HfO_2$ and polyelectrolyte bilayers.

**S10. Internal quantum efficiency spectra**

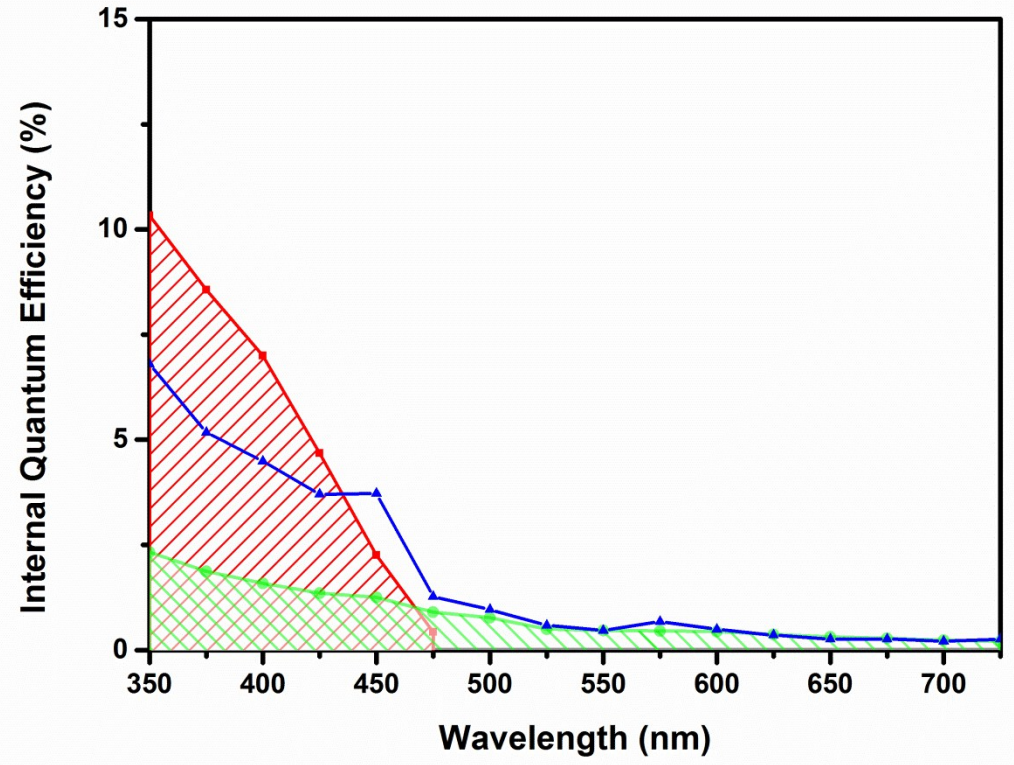


**Figure S10.** Internal quantum efficiency (IQE) spectra of the CdTe NC-based PNS (red), CdHgTe NC-based PNS (green) and tandem CdTe-CdHgTe NC-based PNS (blue) as a function of the wavelength while no external bias is applied across the PNS devices. This figure shows the agreement between the IQE spectra, and the absorbance spectra of the NCs and the top semi-transparent contact, suggesting that the entirety of photoresponse spectral profile is from excitation of the NCs and subsequent exciton dissociation when the light is incident from the top.

**S11. Current density-voltage characteristics of the tandem PNS under dark conditions**

The J-V characteristic under the dark conditions indicates very low dark current densities passing through the device, due to the dielectric layer blocking the charges.

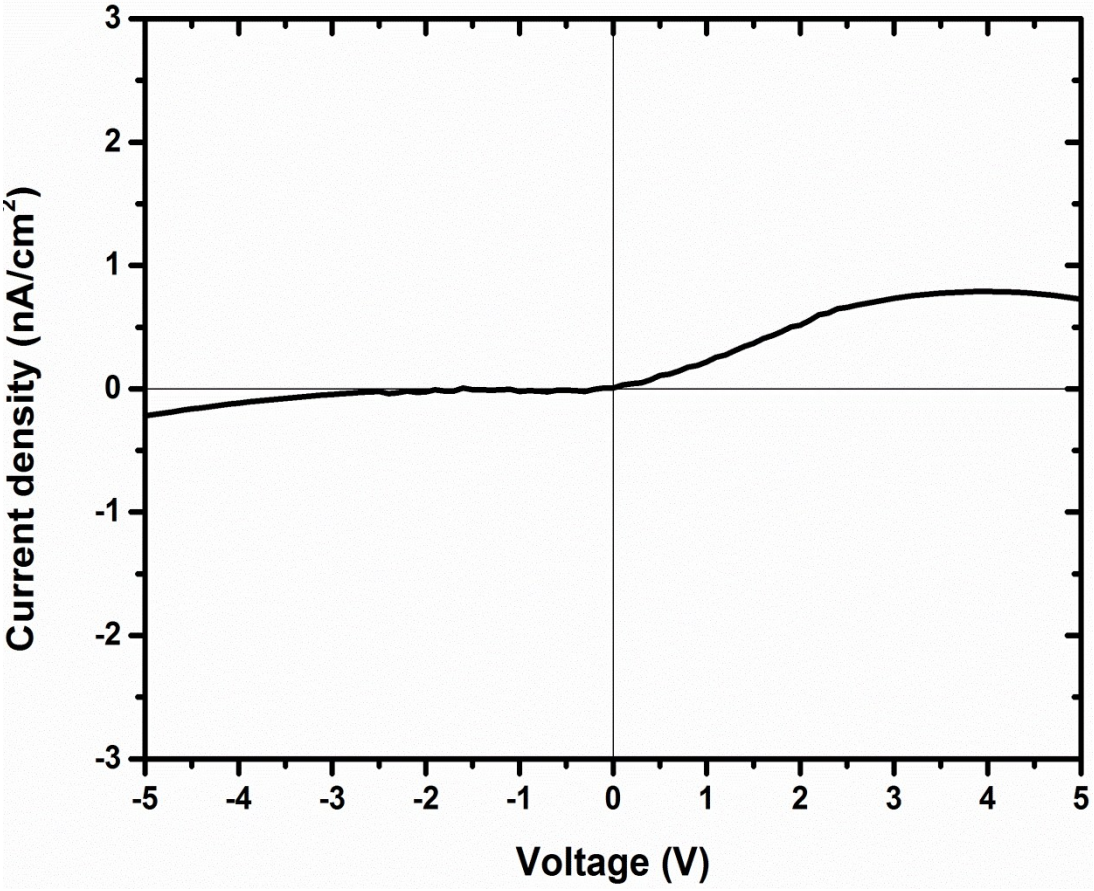


**Figure S11.** Current density-voltage characteristics of the tandem PNS under the dark condition. The figure indicates very low dark current densities passing through the device, because of the presence of blocking dielectric film (which is made of 50 nm hafnium dioxide ($HfO_2$) deposited by atomic layer deposition and four bilayers of polydiallyldimethylammonium chloride-polysodium 4-styrenesulfonate (PDDA-PSS)).

**S12. Mechanical bending test on the tandem PNS**

The flexible PNS can be bent over a 3.5 mm radius of curvature with device performance degradation to the half of the unbent configuration. With further decreasing the radius of curvature, the photovoltage buildup suddenly decreased due to crack formation, especially in the ITO coating. In other words, by a progressive decrease in the $R_c$ value, the electrical resistance of the ITO-coated Kapton exhibits a sudden increase. Subsequently, these devices cannot be operated anymore.

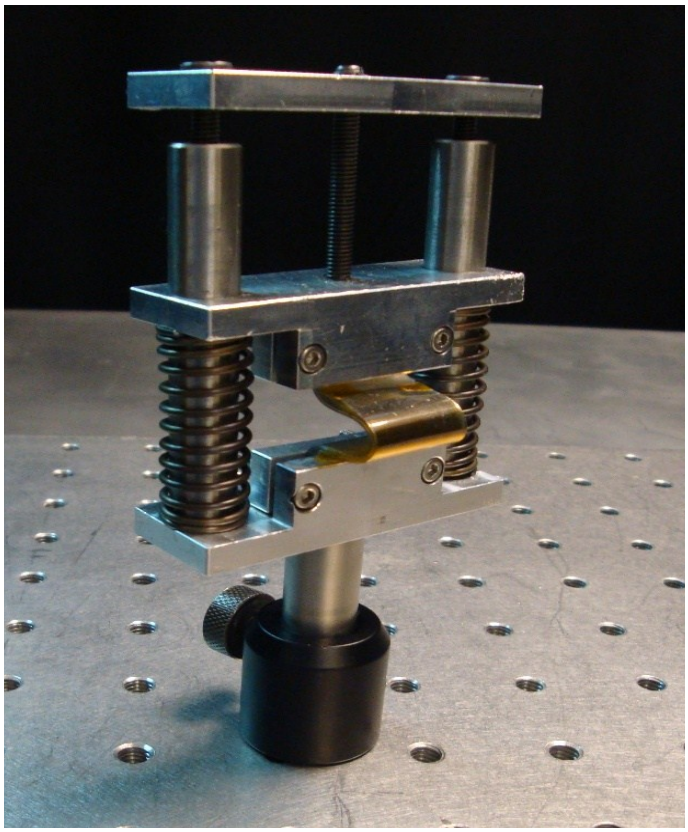

**Figure S12.** Photograph of the device under mechanical bending test.

**References**


1. D. K. Kim, Y. Lai, B. T. Diroll, C. B. Murray, C. R. Kagan, *Nat. Commun.,* 2012, **3**, 1216.

2. E. M. Likovich, R. Jaramillo, K. J. Russell, S. Ramanathan, V. Narayanamurti, *Adv. Mater.,* 2011, **23**, 4521.

3. A. Shavel, N. Gaponik, A. Eychmüller, *Eur. J. Inorg. Chem*., 2005, 3613.

4. G. Decher, *Science,* 1997, **277**, 1232.

5. S. Akhavan, A. F. Cihan, B. Bozok, H. V. Demir, *Small,* 2014, **10**, 2470.